Available online at www.sciencedirect.com
ScienceDirect
Chemical Physics Letters 437 (2007) 229–232
CHEMICAL PHYSICS LETTERS
www.elsevier.com/locate/cplett

Interaction between Pt nanoparticles and carbon nanotubes – An X-ray absorption near edge structures (XANES) study

Jigang Zhou [a], Xingtai Zhou [a], Xuhui Sun [a], Ruying Li [b], Michael Murphy [a], Zhifeng Ding [a,*], Xueliang Sun [b,*], Tsun-Kong Sham [a,*]

[a] Department of Chemistry, The University of Western Ontario, London, Ont., Canada N6A 5B7
[b] Department of Mechanical and Materials Engineering, The University of Western Ontario, London, Ont., Canada N6A 5B7

Received 20 November 2006; in final form 18 January 2007
Available online 15 February 2007

Abstract

The interaction between Pt and carbon in Pt nanoparticles (NPs)–carbon nanotubes (CNTs) composite has been investigated with Pt M_3-edge and C K-edge X-ray absorption near edge structures (XANES) recorded in surface-sensitive total electron yield (TEY) and bulk-sensitive fluorescence yield (FLY). XANES in TEY shows that Pt NPs on CNTs have a fcc structure and the white-line features of the XANES strongly support that the crystalline Pt NPs interact with CNTs through synergic bonding involving charge redistribution between C 2p-derived states and Pt 5d bands. Such interaction facilitates the immobilization of Pt NPs on CNT surface without generating oxygenated functional groups.

1. Introduction

The interactions between solid catalysts and supports [1] play a critical role in determining their performances. Pt nanoparticles (Pt NPs) supported on the high-surface-area carbon [2] is a well adopted catalyst. However, it suffers from rapid oxidation of the carbon support and consequently, loses its catalytic ability [3]. Thus, substitute support materials are intensively sought. Among the alternatives, carbon nanotubes (CNTs) [4] are very attractive. Pt or Ru NPs [5–8] supported on CNTs have been utilized as fuel cell catalyst and show great promise in improving catalytic efficiency [6–9] and prolonging operation lifetime [3].

Although the catalyst-support interaction in the NPs–CNTs composite is crucial to the understanding of the functionality of the catalyst, the nature of the interactions still remains in question because of relatively limited analysis methods. X-ray photoelectron spectroscopy (XPS) [10] and extended X-ray absorption fine structures (EXAFS) [11] have been used to study the interactions. However, direct spectroscopic evidence for the interaction between Pt and carbon is still lacking. A novel route was recently developed to prepare Pt NPs deposited directly on silane polymerized CNTs, which has excellent catalytic ability [5]. For such a system, it is again as difficult to evaluate the interaction between Pt NPs and CNTs, as in the case of interactions between Pt NPs and oxygen-functionalized CNTs [6,11,12]. In this work, we report a study of Pt NP–CNT interactions using X-ray absorption near edge structures (XANES).

XANES measures the modulation of the absorption coefficient at a particular core level of an atom in a chemical environment. XANES has been successfully applied to investigate the chemical bonding, electronic structure and surface chemistry [13–16]. It is element specific and can also be sensitive to either the surface or the bulk of the specimen depending on the edge and the detection schemes. Here we apply C K-edge and Pt M_3-edge XANES to elucidate the

* Corresponding authors. Fax: +1 519 661 3022 (Z. Ding, T.-K. Sham); +1 519 661 3020 (X. Sun).
E-mail addresses: zfding@uwo.ca (Z. Ding), xsun@eng.uwo.ca (X. Sun), sham@uwo.ca (T.-K. Sham).

0009-2614/$ - see front matter © 2007 Elsevier B.V. All rights reserved.
doi:10.1016/j.cplett.2007.02.026

interactions between Pt NPs and CNTs in our Pt NPs–CNTs composite system. Investigation of such interactions will help understand the details underlying the improved performance and factors governing the stability.

2. Experimental

We once used carbon paper as substrates to grow multi-walled carbon nanotubes (MWCNTs) [5,17]. In this study, however, we grew scrolled MWCNTs on a stainless steel mesh instead of carbon paper to avoid the carbon signal from the substrate. The synthesis was performed in a specifically designed chemical vapor deposition (CVD) reactor as reported previously [5,17]. This reactor takes advantage of the fact that the stainless steel mesh is the most resistive part of the electrical circuit. Therefore, the mesh can be heated by Joule effect, up to 800 °C. Under this temperature, ethylene gas can be decomposed on Ni–Co catalyst nanoparticles to grow nanotubes (CNTs) on the mesh.

The synthesis of Ni–Co nanoparticles on the mesh has been described elsewhere [18]. In this method, a key step is the use of a commercially available silane derivative (2-(4-chlorosulfonylphenyl) ethyl trichlorosilane, United Chemical Technologies) solution (1% silane + 6% water + 93% ethanol) to obtain uniformly distribution of Ni–Co catalyst on the mesh without any pretreatments. In fact, a hydrolysis of the silane results in forming a sulfonic acid–silicate and permitting the exchange of H^+ for Co^{2+} and Ni^{2+} ions. Upon reduction in hydrogen at 580 °C for 15 min, the latter ions are the precursors of the Co–Ni particles.

The same procedure for preparing Ni–Co NPs on the mesh was employed to deposit Pt NPs onto CNTs [5], but using $PtCl_2$ as the Pt precursor. The composite thus obtained, is denoted Pt NPs–CNTs. The loading of Pt NPs in such composite was estimated to be 5 wt% [5]. Silane impurity should be very low according to the procedure.

A Hitachi-9000 NAR transmission electron microscope (TEM) operated at 300 kV, and a LEO 1540 scanning electron microscope (SEM), operated at 3 kV, were employed to characterize the structure and morphology of the CNTs and Pt NPs–CNTs.

The C K-edge XANES spectra were obtained at the high energy resolution monochromator (HERMON) beamline (resolution: ~0.3 eV) and the Pt M_3-edge spectra at the Canadian DCM beamline, respectively, at the Synchrotron Radiation Center (SRC), University of Wisconsin-Madison. Commercial MWCNTs (MWCNTs), highly ordered pyrolytic graphite (HOPG) and Pt metal (Aldrich) were also examined as references. XANES spectra were recorded in both total electron yield (TEY) and X-ray fluorescence yield (FLY) modes using specimen current and a multichannel plate detector, respectively. Data were normalized to the incident photon flux. After background correction, the spectra at C K-edge and Pt M_3-edge are normalized to the edge jump, the difference in absorption coefficient just below and at a flat region above the edge (300 eV and 2708 eV for C and Pt, respectively).

3. Results and discussion

TEM image of CNTs in Fig. 1a shows that they have uniform diameter of ~30 nm. The CNTs obtained have a scrolled structure, in which each layer of the tubes is generated by the scrolling of a graphene sheet [19]. Although the concentric structure of CNTs is often observed, the scrolled nanotubes were also reported recently [20,21]. SEM image of the Pt NPs–CNTs composite in Fig. 1b shows that some tubes formed bundles during the Pt NPs deposition. General deposition routes usually require the pre-oxidation of the CNT' surfaces [6,10,11] to generate surface defects, which then allow the localization of the Pt NPs. The advantage of the present technique is that the adsorption of Pt NPs on pristine CNTs avoids the surface oxidation process, yet still generates finely dispersed Pt NPs. As shown in Fig. 1c, small Pt NPs with a diameter around 2 nm are finely dispersed onto the surface of CNTs.

The Pt M_3-edge XANES of the Pt NPs–CNTs and Pt metal are shown in Fig. 2. The identical absorption features confirm the crystalline characteristic of Pt NPs as that Pt metal [15]. The Pt M_3 edge XANES, like that of the Pt L_3 edge, probes the unoccupied densities of state of primarily Pt $5d_{5/2}$ and $5d_{3/2}$ characters as well as the crystal struc-

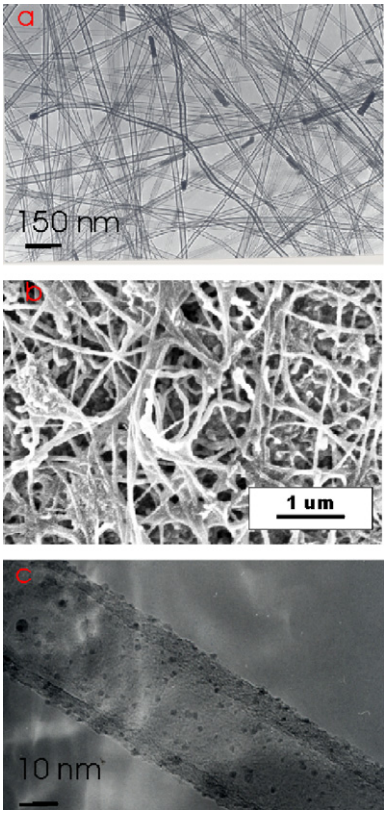

Fig. 1. (a) TEM image of CNTs grown on steel mesh; (b) SEM image of the Pt NPs-CNTs composite; (c) TEM image of one CNT with Pt NPs deposited on it.

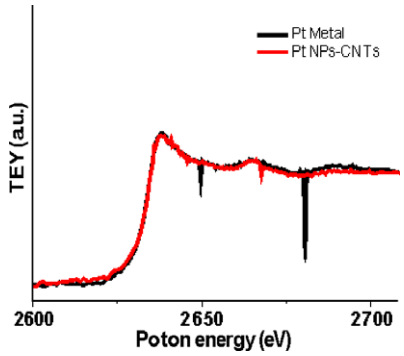

Fig. 2. Pt M_3-edge XANES of the Pt NPs-CNTs composite and Pt metal.

ture. Since the Pt d band is not completely filled, the 3p–5d dipole transition results at the threshold a sharp peak known as whilteline. The area under the whiteline is proportional to the densities of states of 5d holes in the Pt d band that crosses the Fermi level. The oscillations beyond the whiteline are the multiple scattering resonances, which are characteristic of the crystal structure of fcc Pt (hcp and bcc lattice would yield a distinctly different pattern) [22].

A close examination of the absorption white lines shown in the Fig. 2 reveals a very small reduction in intensity in the Pt NPs XANES relative to that of Pt metal. This is surprising since a more intense whiteline is often observed and expected in Pt NPs supported on nano Si substrates such as porous silicon due to Pt NP–Si oxide interactions which withdraw d charges from Pt [23]. Since the M_3-edge XANES whiteline involves electron transition from Pt $3p_{3/2}$ to 5d unoccupied states, the unchanged/slightly reduced density of states of 5d holes (unoccupied) of Pt NPs inferred from the whiteline intensity suggests that charge redistribution between the environment and the Pt d orbitals either has not taken place or has taken place in a synergic manner (charge compensation). In other words, Pt in Pt NPs on CNTs either has not lost d electron charge, in contrast to the observation of Pt NPs on porous silicon [23], or has lost d charge through one d channel but gained it back through another d channel. It appears that this discrepancy between Pt on porous Si and Pt on CNT arises from the difference in the nature of the interactions. We show below that the presence of unsaturation in the graphene sheets (delocalized π orbitals) makes synergic bonding possible. Interestingly, Pt L edge EXAFS did not show much structure change [24], which agrees with our observation.

Fig. 3 plots the C K-edge XANES spectra in TEY for HOPG, commercial MWCNTs, as-prepared CNTs and the Pt NPs–CNTs. The photon energy is calibrated to the C 1 s to π^* transition of HOPG at 285 eV. In the TEY mode, which is surface-sensitive, three main peaks are clearly displayed at ~285 eV, ~287 eV or ~288 eV and ~291 eV for all samples. These can be attributed to the transitions from C 1s to unoccupied states of C–C π^*, C–H σ^* or C–O σ^* and C–C σ^* characters [14,16], respectively. The CNTs and Pt NPs–CNTs exhibit a C–O σ^* feature

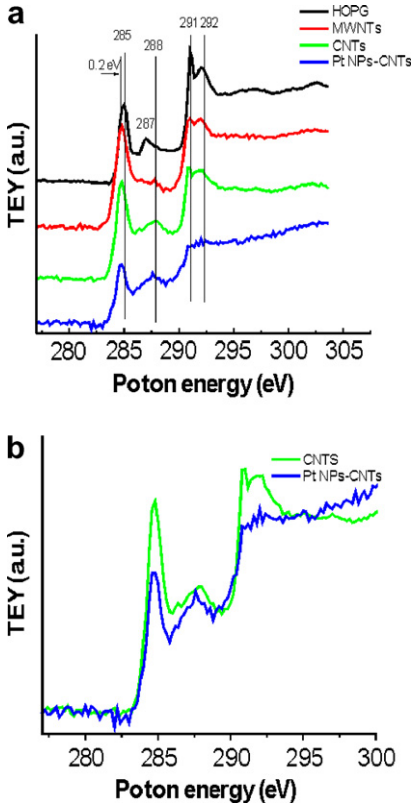

Fig. 3. C K-edge TEY XANES of HOPG, commercial MWCNTs, as-prepared CNTs and the Pt NPs–CNTs composite (a) and detailed comparison of CNTs and the Pt NPs–CNTs composite.

while HOPG shows a C–H σ^* transition. The C–O feature in scrolled CNTs is expected since the edge plane is easily oxidized. It must be noted that this C–O σ^* transition is only observed in TEY and is absent in FLY as shown in Fig. 4. This observation suggests that the C–O peak is only associated with the surface of CNTs. The sharp peaks in TEY become blurred in FLY, more noticeable in HOPG and least noticeable in Pt NPs–CNTs. In fact the FLY of Pt NPs–CNTs exhibits a better defined σ^* resonance at ~291 eV. The more blurry FLY appearance in HOPG is attributable to self-absorption of the fluorescence X-rays

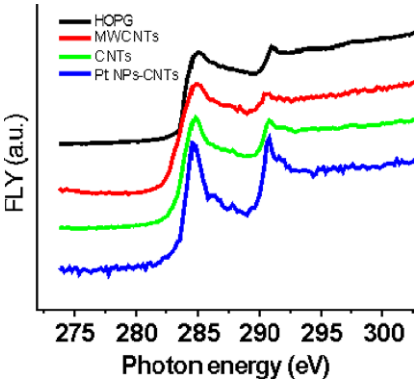

Fig. 4. C K-edge FLY XANES of HOPG, MWCNTs, the prepared CNTs and the Pt NPs–CNTs composite.

by the specimen and is related to the sample's thickness. Ideally, when the sample is thin (less then one absorption length, for example), TEY and FLY XANES should be very similar. In fact, the TEY and FLY XANES for Pt NPs–CNTs show that there is a noticeable interaction between the Pt NP and the surface of CNTs, while the inner graphene layers of the CNTs remain relatively intact.

All CNTs have C–C π^* transition energy down shifted by ~0.5 eV and have broader transition peaks relative to that of HOPG. This can be understood by considering that CNTs are formed through rolling of a graphene sheet, which will make π orbital more delocalized [13]. Other than these two differences, all the absorption features between HOPG and CNTs are in excellent agreement. This observation confirms the graphite feature of CNTs under investigation. Therefore good electric conductivity for CNTs and Pt NPs–CNTs is expected. The absence of a sharp σ^* transition at ~291 eV in the TEY mode can be attributed to Pt NPs–CNTs interactions (see below) as noted above. The FLY XANES shows a sharp σ^* resonance, indicating that the CNTs have relatively little defects in the inner layers [13]. The low defect density will also benefit CNTs with longer operation life in fuel cell with their conductivity, chemical stability and mechanic strength.

Since C K-edge investigates the unoccupied molecular orbitals with carbon p characters, the area beneath the resonance is proportional to the unoccupied DOS. The reduction of DOS of p character in Pt NPs–CNTs relative to that of CNTs in Fig. 3b provides the evidence that charge transfer from environment, the Pt NPs, to C 2p-derived states has occurred. It is conceivable that the 5d levels in Pt, which is not completely filled, accepts electron from CNTs to form σ bond and back-donates electron to the π^* of the CNTs reducing the DOS of unoccupied 2p-derived states but the d charge at the Pt site changes very little. This synergic bonding is common in noble metals [23]. It explains the relative small change in whiteline intensity, hence DOS of Pt in Fig. 2. Similar back-bonding process has been observed by XPS in Ni nanoparticle interaction with HOPG [25]. In the present system, it is conceivable that Pt nucleation prefers the edge planes, which are characteristic of scrolled CNTs. Such site-selective nucleation has been reported in Pt NPs deposited on HOPG [26,27]. The bonding scheme should contribute to the formation of fine-sized Pt NPs, the good dispersion of Pt NPs as well as the immobility of Pt NPs on CNTs, which will prevent lateral diffusion of Pt NPs, especially under fuel cell operation conditions.

In summary, we have prepared fine Pt NPs decorated CNTs and applied XANES at the C K-edge and Pt M_3-edge to elucidate the interactions between crystalline Pt NPs and CNTs. The interactions involve C 2p-derived states and Pt 5d characters. We demonstrated the advantage of XANES in clarifying the interactions between catalyst and its supports. It is anticipated that XANES will be widely used in the characterization of catalyst-support systems.

Acknowledgements

The authors thank Drs. F. Heigl and A. Jurgensen at the CSRF at SRC, University of Wisconsin-Madison, for their technical assistances, Dr. Todd Simpson of the Nanofabrication Lab at the University of Western Ontario (UWO) for his help on the SEM. This work is based in part upon research conducted at SRC, which is supported by the National Science Foundation under Award no. DMR-0537588. The work at UWO was supported by NSERC, OPC, CFI, OIT, PREA, ERA, EMK and CRC.

References

[1] R.T.K. Baker, S.J. Tauster, J.A. Dumesic, Strong metal support interactions, American Chem. Soc., Washington, D.C., 1986.
[2] K. Lee, J. Zhang, H. Wang, D.P. Wilkinson, J. Appl. Electrochem. 36 (2006) 507.
[3] Y. Shao, G. Yin, Y. Gao, P. Shi, J. Electrochem. Soc. 153 (2006) A1093.
[4] S. Iijima, Nature 354 (1991) 56.
[5] X. Sun, R. Li, D. Villers, J.P. Dodelet, S. Desilets, Chem. Phys. Lett. 379 (2003) 99.
[6] Y. Xing, J. Chem. Phys. B 108 (2004) 19255.
[7] J.M. Planeix et al., J. Am. Chem. Soc. 116 (1994) 7935.
[8] R. Yu et al., Chem. Mater. 10 (1998) 718.
[9] W. Li et al., Carbon 40 (2002) 791.
[10] R.V. Hull, L. Li, Y. Xing, C.C. Chusuei, Chem. Mater. 18 (2006) 1780.
[11] Y. Xing, L. Li, C.C. Chusuei, R.V. Hull, Langmuir 21 (2005) 4185.
[12] B.C. Satishkumar, E.M. Vogl, A. Govindaraj, C.N.R. Rao, J. Phys. D: Appl. Phys. 29 (1996) 3173.
[13] Y.H. Tang, T.K. Sham, Y.F. Hu, C.S. Lee, S.T. Lee, Chem. Phys. Lett. 366 (2002) 636.
[14] Y.H. Tang et al., Appl. Phys. Lett. 79 (2001) 3773.
[15] P. Zhang, X. Zhou, Y. Tang, T.K. Sham, Langmuir 21 (2005) 8502.
[16] S. Banerjee, T. Hemraj-Benny, M. Balasubramanian, D.A. Fischer, J.A. Misewich, S.S. Wong, Chem. Commun. (2004) 772.
[17] X. Sun, B.L. Stansfield, J.P. Dodelet, S. Desilets, Chem. Phys. Lett. 363 (2002) 415.
[18] X. Sun, R. Li, G. Lebrun, B.L. Stansfield, J.P. Dodelet, S. Desilets, Int. J. Nanoscience 1 (2002) 223.
[19] X. Sun, R. Li, B. Stansfield, J.-P. Dodelet, G. Ménard, S. Désilets, Carbon 45 (2007) 732.
[20] G. Xu, Z.-C. Feng, Z. Popovic, J.-Y. Lin, J.J. Vittal, Adv. Mater. 13 (2001) 264.
[21] W. Ruland, A.K. Schaper, H. Hou, A. Greiner, Carbon 41 (2003) 423.
[22] T.K. Sham, S.J. Naftel, I. Coulthard, J. Appl. Phys. 79 (1996) 7134.
[23] I. Coulthard, T.K. Sham, Solid State Commun. 105 (1998) 751.
[24] I. Robel, G. Girishkumar, B.A. Bunker, P.V. Kamat, Appl. Phys. Lett. 88 (2006) 073113.
[25] D.Q. Yang, E. Sacher, J. Chem. Phys. B 109 (2005) 19329.
[26] D.Q. Yang, B. Hennequin, E. Sacher, Chem. Mater. 18 (2006) 5033.
[27] D.Q. Yang, G.X. Zhang, E. Sacher, M. Jose-Yacaman, N. Elizondo, J. Chem. Phys. B 110 (2006) 8348.